Fluid interface calorimetry

Pablo Fernandez Garrido, Margarida Bastos, Adrián Velázquez-Campoy, Philippe Dumas, Ángel Piñeiro

Journal of Colloid and Interface Science 596 (2021) 119–129

Contents lists available at ScienceDirect

Journal of Colloid and Interface Science

journal homepage: www.elsevier.com/locate/jcis

Regular Article

Fluid interface calorimetry

Pablo F. Garrido [a,*], Margarida Bastos [b], Adrián Velázquez-Campoy [c,d,e,f,g], Philippe Dumas [h], Ángel Piñeiro [a,*]

[a] Departamento de Fisica de Aplicada, Facultade de Fisica, Universidade de Santiago de Compostela, E-15782 Santiago de Compostela, Spain
[b] CIQ-UP, Departamento de Quimica e Bioquimica, Faculdade de Ciencias da Universidade do Porto, R. Campo Alegre 687, P-4169-007 Porto, Portugal
[c] Institute of Biocomputation and Physics of Complex Systems (BIFI), Joint Units IQFR-CSIC-BIFI, and GBsC-CSIC-BIFI, Universidad de Zaragoza, Zaragoza 50018, Spain
[d] Department of Biochemistry and Molecular and Cell Biology, Universidad de Zaragoza, 50009 Zaragoza, Spain
[e] Aragon Institute for Health Research (IIS Aragon), 50009 Zaragoza, Spain
[f] Biomedical Research Networking Centre for Liver and Digestive Diseases (CIBERehd), 28029 Madrid, Spain
[g] Fundacion ARAID, Government of Aragon, 50018 Zaragoza, Spain
[h] IGBMC, Dept of Integrative Biology, Strasbourg University, F67404 Illkirch CEDEX, France

GRAPHICAL ABSTRACT

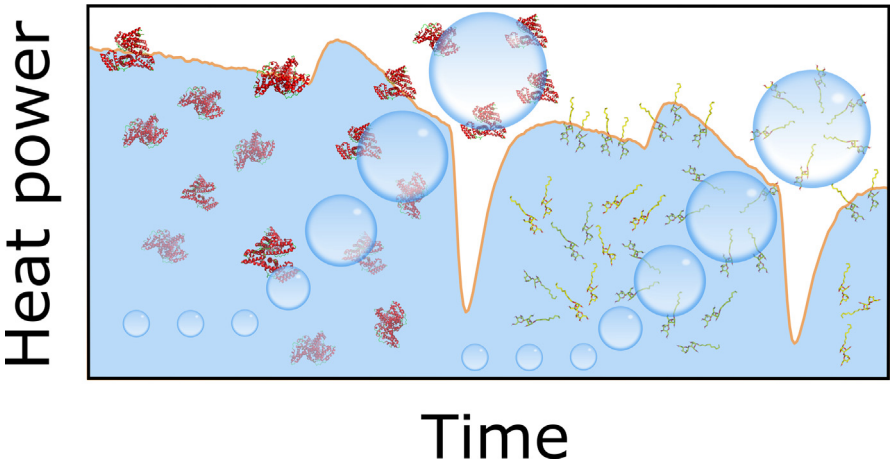

ARTICLE INFO

Article history:
Received 17 February 2021
Revised 15 March 2021
Accepted 16 March 2021
Available online 22 March 2021

Keywords:
Interfaces
Calorimetry
Adsorption
Isothermal Titration Calorimetry
Surface Tension

ABSTRACT

Hypothesis: Amphiphilic molecules spontaneously adsorb to fluid polar-nonpolar interfaces. The time-scale of such adsorption depends on the molecular size and structure of the solute. This process should be accompanied by a power heat exchange that could be detected by commercial isothermal calorimeters.

Experiments: Air is injected in the bulk of different aqueous solutions contained in the sample cell of an isothermal titration calorimeter. The formation of the resulting bubbles leads to a liquid/air interface to which the solute molecules spontaneously adsorb. Continuous injection experiments to produce multiple bubbles as well as experiments with static bubbles stand from the capillary tip, aiming to observe slow adsorption processes, were performed.

Findings: The power associated with the formation, growth and release of air bubbles in different liquids was measured. Different independent contributions that can be associated to the pressure change in the

* Corresponding authors.
E-mail addresses: Pablo.Fernandez@usc.es (P.F. Garrido), Angel.Pineiro@usc.es (Á. Piñeiro).

https://doi.org/10.1016/j.jcis.2021.03.098

gas phase, the evaporation-condensation of the solvent, the increase of interfacial area, the change in the heat capacity of the sample cell content, and the release of the bubble were observed. The periodic pattern produced by the continuous injection of air at a constant rate is used to determine the surface tension of different liquids, including solutions of different molecules and (bio)macromolecules.

1. Introduction

Isothermal titration calorimetry (ITC) is a highly sensitive and versatile technique aimed for the characterization of molecular interactions. No labelled or chemically modified compounds are required to perform the measurements, the molecules do not need to be fixed to any artificial substrate, and the experiments are directly performed in solution, mimicking the conditions where the target molecules are typically expected to carry out their native function [1]. Well-designed ITC experiments can provide thermodynamic information on systems that interact in complex ways, including molecular recognition processes coupled to aggregation and/or dissociation events. The variety of systems that can be characterized by calorimetric methods is not restricted by the size or the structure of the involved molecules or molecular aggregates. Competitive multivalent interactions, dissociation-aggregation mechanisms, protein or polymer conformational changes induced by the binding of small molecules, and the interaction between vesicles, liposomes or artificial nanoparticles with proteins, peptides and other molecules have been characterized by calorimetric methods [2–4]. Simpler mechanisms like the dissociation of dimeric proteins or the aggregation of small molecules giving micelles have also been studied by ITC [5,6]. Typically, thermodynamic parameters such as the enthalpy and the association (dissociation) constants are obtained from the analysis of ITC experiments, from which the Gibbs energy and the entropy contributions to the studied process can be calculated. Further, a method to obtain kinetic information, taking advantage of the analysis of the raw data provided by ITC, has been published [7] and made easy to use [8,9]. Advanced computational tools designed to analyze a large variety of calorimetric experiments, and aimed to the characterization of interaction mechanisms, including also kinetic parameters for one-step interactions, are publicly available [10–13].

The use of ITC in the study of intermolecular interactions has been somewhat hindered by the amount of sample required for each measurement, typically larger than in the case of other techniques such as Surface Plasmon Resonance (SPR) or MicroScale Thermophoresis (MST). However, the important reduction of cell volume in the last generation instruments, together with the abovementioned features of ITC, and the fact that it is the only technique that can provide full thermodynamic characterization of the process under study from a single experiment, has positioned ITC as the best alternative for the characterization of a large variety of inter- and intra- molecular interactions. As such, calorimetric studies of physicochemical events provide fundamental information for their full characterization. Noteworthy, specific experimental and theoretical calorimetric methods have been developed to assess the heat of adsorption of gases and liquids onto solids [14,15]. Despite the wide range of calorimetric applications, to the best of our knowledge, no attempts have yet been made to measure the heat of molecular adsorption or surface formation at fluid interfaces. Such measurements would require to follow the formation of new surface in real time. The thermodynamic and kinetic characterization of the interaction between different fluid phases would facilitate the understanding of a number of applications, mainly those related with foams, interfacial (bio)-films, adsorption mechanisms and the characterization of liquid/-vapor or liquid/liquid interfaces.

Several techniques are available to assess thermodynamic, structural and kinetic properties of molecules at interfaces, such as surface tension, ellipsometry and different microscopy and spectroscopy approaches [16–19]. Surface tension (γ) is the most basic of these properties and different methods are available to determine its value for a given liquid sample. The correlation between the surface tension and the maximum pressure of a bubble attached to the tip of a capillary while it is growing in a liquid upon air injection is one of the most classical approaches, the so called "maximum bubble pressure method" [16]. This method is well suited to be implemented in typical isothermal titration calorimeters with none or just slight modifications in the instruments. The injection of air into the calorimeter measurement cell at controlled pressure and/or flow rate is expected to allow quantitative surface tension measurements of liquid samples, while simultaneously determining the corresponding power exchange upon air injection. No other experimental method can directly obtain the dependence of the measured heat of adsorption to fluid interfaces on the molecular composition of the studied solution. In the present paper we show that: i) the power corresponding to the injection of air and consequent formation of bubbles in a liquid sample can be easily assessed by using standard ITC instruments; ii) these experiments clearly distinguish different liquids; and iii) if water is the solvent, different concentrations of cosolvents, surfactants and even proteins can be differentiated. The experimental procedure required to create and analyze air/liquid bubbles in a calorimetric cell, with no modifications in the instrument, as well as the main variables that can affect the measurements, are described in detail. Further to this, several potential applications of this method and some modifications in the experimental setup are proposed, to improve the results at the quantitative level.

2. Materials and methods

2.1. Materials

Ultrapure water (Elix 3 purification system, Milipore Corp.), ethanol (99.8% min. purity from Panreac) and cyclohexane (99.7% min. purity from Honeywell) were used in the experiments. All liquids were degassed trough vacuum prior to the ITC measurements. Decyl-β-D-maltopyranoside ($C_{10}G_2$) was purchased from Anatrace, Bovine Serum Albumin (BSA) was purchased from Sigma and Ethylammonium Nitrate (EAN) was purchased from Iolitec. All the compounds were used as received, without further purification.

2.2. Selection of the instrument

We aimed at measuring the thermal power accompanying the formation, growing and releasing of air bubbles. The power signal involved in these experiments is expected to be weak and to change quickly, so we need an instrument with high sensitivity and short response time. In this work, the injection system of current ITC instruments was employed to achieve our aim. The shape and volume of the sample cell and the radius of the capillary used for the injection are key parameters for these measurements since

the bubble should be large enough to be detectable and not too large to avoid contact with the cell walls. A range of apparently suitable ITC instruments are commercially available. Nowadays, two main companies manufacture ITCs: TA-Instruments and MicroCal/Malvern Panalytical. The former uses cylindrical-shaped cells while the later uses coin-shaped cells, whereas the range of available volumes are similar (for volumes up to 1400 μL). Nevertheless, fundamental differences between these branches exist as regarding the way the power is measured, the feedback and the stirring systems. These differences have an impact in the detected power signal that should be taken into account when interpreting and analyzing the raw data. Since we are interested in the kinetics of the bubble formation process, for our experiments the power sensitivity is more relevant than the minimum power detection. However, even though ITC instruments are well suited to monitor kinetic signals [7,20,21], they usually aim at the thermodynamic characterization of the studied process, and therefore the latter parameter is typically considered more important than the former. Fortunately, the short-term noise (STN), which is an estimation of the power fluctuations when the sample is thermally stabilized before the start of the titration experiment, is typically provided by the manufacturers in the technical specification sheet of the instrument and can be taken as an estimation of the power sensitivity. In present work we tested seven different titration calorimeters (see Table 1).

During our preliminary tests, all the instruments described in Table 1, except the commercial version of the TAM III, were able to detect the signal corresponding to the air injection/bubble formation. As stated above, the volume of the bubble, which depends directly on the diameter of the capillary of the injection system, should be large enough to produce a detectable power signal (larger than the STN) and the cell volume should also be not too large to ensure no contact between the bubble and the cell wall. Note that the power due to bubble formation could be magnified by optimizing the air injection rate and the diameter of the capillary. The injection rate is normally accessible from the control software. It should be slow enough so that the characteristic response time of the instrument allows observing the kinetic signal but also fast enough to produce a measurable power distinguishable from the baseline. Thus, the instrumental response time is also a key feature for these experiments. It is worth commenting that the response time depends on the sample solution due to the change in the heat conductivity and heat capacity arising from the different compositions and interactions with the sample cell [23]. So special care should be taken to keep the cell extremely clean to prevent changes in the response time.

ITC instruments usually contain a stirring system to guarantee that the solution in the sample cell is homogeneous in a short time. In our experiments the stirrer had to be disconnected or even removed to allow the formation of the bubble. In all experiments reported in this work, the standard injection system of the corresponding instrument was employed to introduce the bubbles in the sample cell. We just connected the clean and dry syringe, filled with air at atmospheric pressure, to the ITC and injected the air at a controlled rate. It is important to stress that the pressure of the air contained in the syringe will not be constant through these experiments, as it will be discussed below. Finally, we would call the attention to the fact that using this method a large number of bubbles can be spontaneously formed during a single experiment.

The signal in the VP-ITC in our preliminary tests was clearer and more reproducible than that from the other instruments, probably due to its higher specific sensitivity (lower STN to cell-volume ratio). Therefore, we decided to focus on the VP-ITC for the experiments production and analysis. This is due to the combination of its geometrical features, specific sensitivity and also to the fact that we have access to three different versions of this instrument (see Table 1) and we can assess the reproducibility of the data using them. No modification at all in the instruments was performed for any of the measurements reported in the present work.

3. Bubble formation in VP-ITC

As explained above, the bubbles were created in the ITC sample cell using the own injection system of the instrument. Special care was taken with the cleaning and with the connections of the syringe (plunger and positioning of the syringe in the instrument for the experiment and connection for the installation of the homemade manometer as will be explained later) to prevent air leakages. Once a specific injection rate is set in the control software, the bubbles are spontaneously created in the sample cell. Depending on the composition of the solution in the sample cell, between 10 and 60 bubbles are typically created in an experiment using a syringe of 200 μL.

Standard ITC experiments consist in sequential small injections of one liquid solution into another of different composition. In the calorimeter used, the power supplied to the reference cell triggers the feedback power on the sample cell, aimed at minimizing the difference in temperature between the sample and the reference cells, and thus the feedback power on the sample cell is registered, and the integral of the signal perturbation upon each injection is plotted as a function of the concentration ratio of the involved compounds in order to perform a thermodynamic analysis. The recovering of a stable baseline is important to get a reasonable estimation of the heat exchanged during each injection. Ideally, the signal corresponding to the injection of bubbles should be performed in a similar way, *i.e.* the volume of air required to form a single bubble should be injected and then we should wait for the recovering of the baseline before pumping more air in the sample cell. However, the compressibility of the injected fluid in our case is much higher than that of standard liquid solutions, and the pressure is significantly changed during the experiment. This, together with the time delay between the event that takes place in the sam-

Table 1
Main features of the ITC instruments employed in the present work. The information of this table was obtained from the corresponding specification sheets provided by the manufacturing companies. For the TA calorimeters, the range of response time and noise arises from the standard volume (maximum) and low volume (minimum) experiments.

Company	ITC	Cell geometry	Cell volume (μL)	Syringe volume (μL)	Short term noise level (nW)	Response time (s)
TA Instruments/Waters	TAM prototype*	Cylindrical	1000–20000	100–2500	–	–
	TAM III	Cylindrical	4000–20000	100–2500	10	–
	Nano ITC	Cylindrical	190–1000	100–250	1.4–2.5	11.0–18.0
	Affinity ITC	Cylindrical	190–1000	up to 250	1.3–2.5	3.3–18.0
MicroCal/Malvern Panalytical	VP-ITC**	Coin shaped	1400	295	2.0	20
	ITC-200	Coin shaped	200	40	0.84***	10
	PEAQ-ITC	Coin shaped	200	40	0.63	8

* This is a non-commercial version of the TAM III, available at MB's Laboratory, University of Porto.
** Three types of VP-ITC (versions 06.05.673, 08.01.255 and 11.10.994) were used in the present work.
*** [22].

ple cell and the registered signal, makes difficult to decide the precise time required for the creation of single bubbles as well as the time required for the injection and for the recovering of the baseline. In all experiments done initially in this way there were indeed uncertainties on what was really happening in the sample cell during what was being considered a single-bubble event: (*i*) creation, growing and release of a bubble; (*ii*) same as (*i*) but followed by the creation of a second bubble in the same injection; (*iii*) release of a bubble that was already created during the previous injection; or (*iv*) release of a mature bubble followed by the formation of another one. For this reason we decided to follow a different strategy, based on a relatively slow but continuous injection, producing sequential bubbles. The main disadvantage of this method is that a stable baseline is not completely reached before the creation of a new bubble. However, if the injection rate is slow enough, a rich kinetic signal can be obtained without much interference from successive bubbles. It is well known that the formation, growing and release of a bubble in the tip of the capillary depends on the air pressure in the syringe, as well as on the surface tension and hydrostatic pressure of the liquid (Fig. 1). Additionally, when introducing the syringe in the instrument to initiate a new experiment, some liquid raises through the needle due to capillarity, what slightly increases the pressure inside the syringe. The balance between these contributions is expected to change with time since the air is continuously being injected and the bubble changes in volume and shape as a response to this pumping.

The injection rate in a VP-ITC can be set by selecting a single injection of a large volume with a specific injection time in the control software. In the present work, a waiting period of 150–300 s was used before starting the air-titration experiments. The total volume of a 200 μL syringe was injected during 9000 s for the slowest experiments and 900 s for the fastest ones. Faster experiments should not be performed as they result in overlapped signal contributions. The baseline was again registered at the end of the titration for at least 300 s.

The formation, growth and release of the bubble depend on the size and shape of the tip of the capillary used to inject the air. In the case of the VP-ITC instruments the capillary used to inject the solution from the syringe in the sample cell has helical-shaped tip, since it is also employed as a propeller to guarantee the homogeneity of the liquid in a typical experiment (Fig. 1). In principle, this geometry would not be ideal for our aims, but as it will be shown later, our results using it were highly reproducible. It is known that a gas bubble reaches its maximum internal pressure when it becomes a hemi-sphere of diameter equal to that of the inner part of the capillary from which it emerges. Beyond this size, as the volume increases the pressure decreases following the Laplace-Young equation ($\Delta P = P_{int} - P_{ext} = 2\gamma/r$ with γ the surface tension and r the radius of the bubble), until the bubble is released [24]. In the case of the VP-ITC, the bubble remains attached to the capillary for a time longer than expected if the needle walls are thinner than its inner diameter, so finally its 'exotic' geometry seems to help to stabilize the bubbles. This is interesting since it contributes to a clearer signal in the instrument.

4. Results for air-water bubbles

Water was chosen as the reference pure liquid to test and optimize the experimental setup. Beyond its immediate availability, its high surface tension gives rise to the formation of large bubbles. In this section, we show how different parameters affect the bubble formation and detection.

4.1. Injection rate dependence

Since two different phases coexist during bubble formation, several events are expected to contribute to the power signal, namely the compression/decompression of the air, vaporization/-condensation effects at the interface, surface creation/destruction, and mechanical perturbations. Another important contribution to

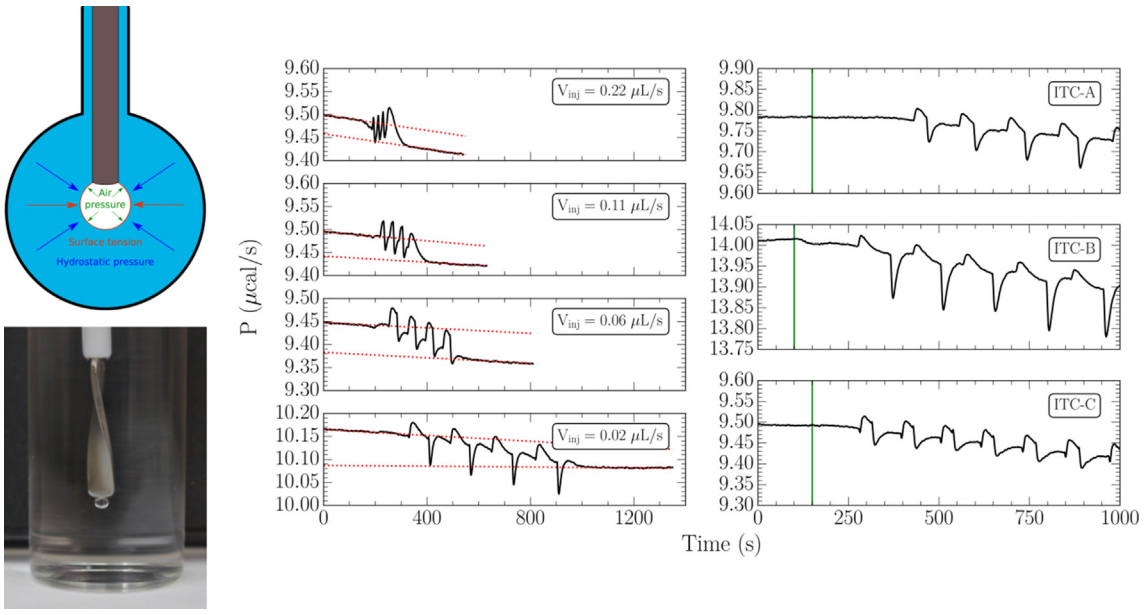

Fig. 1. Left-up: Representation of a bubble inside a calorimetric cell. The arrows indicate the direction of the force due to air pressure (from inside the bubble, pointing outwards) as well as surface tension and hydrostatic pressure (from outside the bubble, pointing inwards). Left-down: picture of the helical-shaped capillary needle of the syringe used with the VP-ITC, immersed in water with a bubble formed and still attached to the tip. Middle: Raw power signal obtained for the injection of air into water at 298 K for four different injection rates: 0.22, 0.11, 0.06 and 0.02 μL/s; corresponding to the injection of 20 μL of air during 90, 180, 360 and 900 s respectively. Red dotted lines represent the baseline linear extrapolation before and after the titration experiment. Right: Comparison of experiments with the same setup (air into water at 0.02 μL/s injection rate and 298 K) using the ITC instruments A, B and C, as indicated by the labels. The green vertical lines indicate the beginning of the injection. (For interpretation of the references to colour in this figure legend, the reader is referred to the web version of this article.)

the signal is the pumping in/out of heat to the cell due to the temperature difference between the environment and the measurement cell. For reasonably slow injections, the heat power contributions of thermodynamic nature associated to the bubble formation should not depend on the injection rate, in contrast to those related to mechanical or external effects. So, the injection rate is expected to affect the time evolution of the thermodynamic contributions to the power signal but not the corresponding areas. Our experiments of air bubbles in pure water revealed that the signal is very clear and reproducible at injection rates lower than 0.06 μL/s, while for faster injection rates different contributions overlap to each other, including those coming from different bubbles (Fig. 1). They also show that the number of bubble formation events that can be observed in the power profile for a given total volume does not depend on the injection rate, as expected, and that the signal is richer in information at slower injection rates.

4.2. Reproducibility of the power profile

The signal is periodic, regardless the injection rate. Independent experiments performed at the same injection rate with the same liquid using the same ITC instrument were practically indistinguishable (Fig. S1). At most, slight differences were visible for the initial power and the slope of the baseline. Less obvious is the tiny difference in the period of the signal between experiments. All together, these differences determine the statistical variability between different measurements using the same instrument.

The same experiment was replicated with three different VP-ITC instruments: 06.05.673, 08.01.255 and 11.10.994 in Table 1; that will be named A, B and C, respectively, from now on. The size of the positive and negative contributions to the power profile is significantly different in each experiment (Fig. 1), producing thus a signal of different shape. However, the number of contributions, as well as the corresponding signs, are the same in all experiments. As expected, the three signals are periodic, but the periods are also significantly different. These differences are similar to those observed when changing the injection rate: the different contributions are more separate from each other in ITC-B than in ITC-A and ITC-C (Fig. 1), which results from a modification of the profile of the signal due to variable overlapping of positive and negative peaks. Also, even when the same injection rate and solvent are employed, the number of bubbles generated within the same time interval was different in each case, assuming that each repeat of the periodic signal corresponds to a bubble. This can only be due to instrument variability, likely at the level of the injection systems and/or the capillaries, since ITC-A and ITC-C were located in the same laboratory and both experiments were performed at the same time using the same sample. Additionally, two other significant differences are observed in ITC-B with respect to ITC-A and ITC-C: a larger negative peak and a higher measured equilibrium power, although the same reference power was used for the three calorimeters, 10 μcal/s. The way that these magnitudes can affect the measurement will be analyzed in the following sections.

4.3. Baseline

For all the data presented in this work there is a systematic negative drift in the baseline during the air-titration experiments. Additionally, in some experiments there is an initial slope in the pre-titration equilibration period, although this is often very small or even negligible (Fig. 1). Repeats of experiments using different initial slopes in the baseline always exhibit a negative drift during the air-titration experiment, with almost identical power profile for each bubble (Fig. S2) This indicates that the initial slope does not significantly affect the results of these experiments and that both contributions to the baseline drift (the initial one and that coming from the air-titration) are independent from each other.

4.4. Reference power

The reference power (RP) is the constant electrical power applied to the reference cell so that the heat absorbed or released in the sample cell (where the bubbles are formed) can be measured through the change in power needed to minimize the difference of temperature between the two cells, through a feedback compensation system. The RP introduces an offset to the baseline and so it changes the maximum power that can be measured without saturation of the instrument. RP significantly affects the slope in the power profile throughout the air-titration experiment (Fig. 2) as well as the shape of the signal corresponding to each bubble, although no clear trends were identified in the variation of such shape. Notably, the period of the signal, and so the bubble size, remains unchanged.

4.5. Temperature dependence

In order to check the impact of the temperature, air-titration experiments with the ITC cells at 283, 293, 298, 310 and 323 K and the lab temperature between 293 and 296 K, were performed (Fig. 2). The temperature is expected to affect the volume of the bubbles by changing the internal air pressure and the surface tension of the liquid-air interface, consequently changing the power signal. Again, a periodic signal with different contributions for each bubble was observed. The main contributions to the signal in the previous experiments at 298 K were a positive peak followed by a negative one (Fig. 1). Notably, the amplitude and even the sign of the first peak clearly changes with temperature, while the second peak remains always negative (exothermic) without a clear trend in amplitude. The evolution of the first peak is clear: it is slightly negative at 283 K, then it becomes slightly positive at 293 K, and the maximum grows in a proportional way to the temperature. This is basically the result of the influence of room temperature on the measurements, as there is no perfect shielding of the calorimetric cell from the surroundings. Repeats of these experiments reproduced the same behavior. On a side note, it is worth to comment that the baseline showed to be less stable at the higher working temperatures.

5. Analysis of air-titration experiments

Our reference experiments are performed using a reference power of 20 μcal/s, an injection rate of 0.02 μL/s (100 μL injected in 4500 s), and an initial and final delays of 300 s. Additionally, the equilibration signal before and after the titration experiment were typically registered for a minimum of 1000 s. A representative experiment is shown in Fig. 3, with the equilibrated signal followed by the periodic profile corresponding to 24 consecutive bubbles and finally the recovery of a constant baseline. The systematic drop of baseline as the air is pumped into the sample cell, together with the clear reproducibility of the power profile corresponding to each bubble are clear in this experiment. The baseline drift during the titration experiment is due to the feedback system used by the employed instrument (VP-ITC from MicroCal), keeping constant the difference of temperature between the reference cell and the sample cell when the temperature of the latter changes due to an exothermic or endothermic process. To detect such temperature fluctuations, a constant power is applied on the reference cell (RP). When both cells contain exactly the same type and amount of liquid, and no stirring is used, the power to be applied to the sample cell to cancel the temperature difference, in the

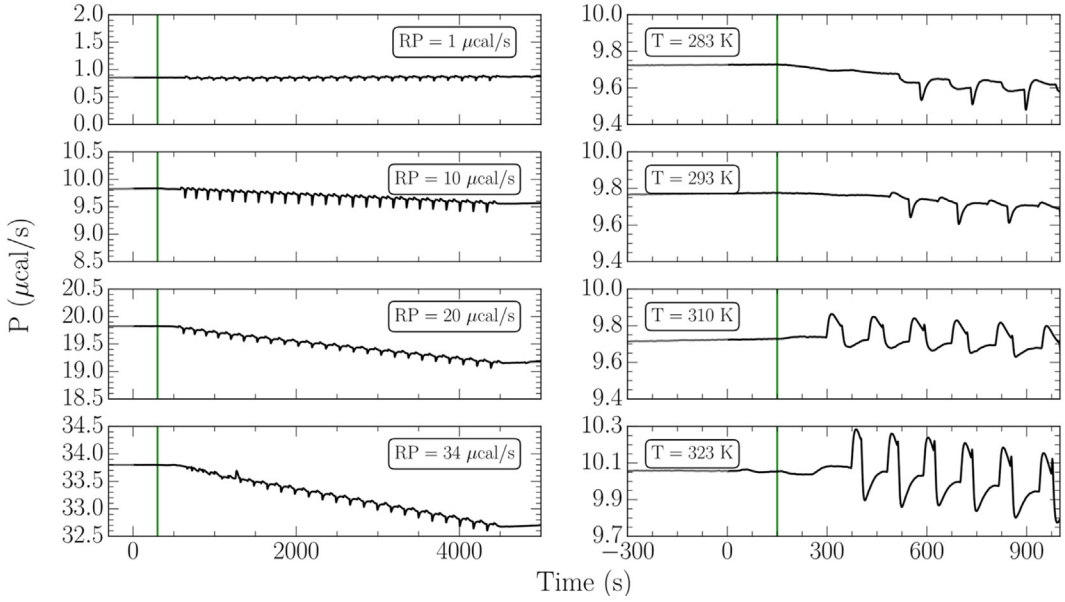

Fig. 2. Left: Power vs time profiles for the injection of air into water at 298 K and 0.02 μL/s, as a function of the reference power (indicated in each plot). Right: Power vs time profile of air-titration experiments for the temperatures indicated in each plot. In all cases, the green vertical lines indicate the beginning of the injection.

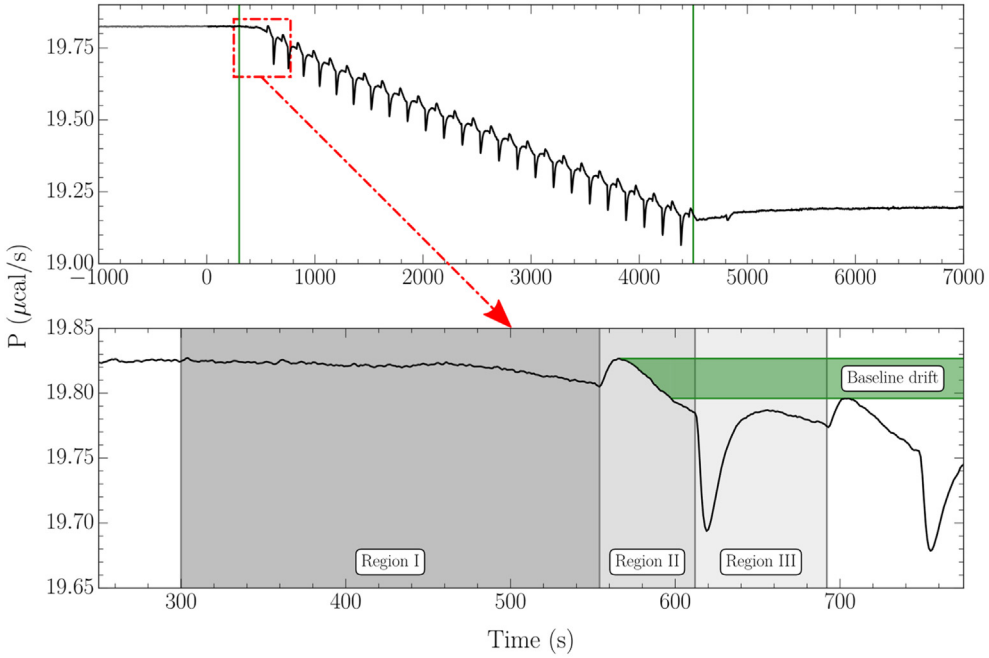

Fig. 3. Experiment corresponding to the injection of air into water using a reference power of 20 μcal/s, an injection rate of 0.022 μL/s (100 μL injected in 4500 s), and an initial and final delays of 300 s. The equilibration signal before and after the titration experiment was registered for 1000 and 2200 s, respectively. The whole titration is shown in the upper plot while the lower one shows the initial amplified region including the profile described by the first two bubbles. The green vertical lines indicate the beginning and end of the air-injection. (For interpretation of the references to colour in this figure legend, the reader is referred to the web version of this article.)

absence of thermal reactions, should be equal to the RP (Fig. 3 during the equilibration period prior to the air-titration). Assuming that the air injected in the sample cell during our experiments remains trapped, and an equivalent volume of liquid is therefore displaced outside the coin-shaped container, the amount of water and thus the total heat capacity of the sample cell decreases upon each injection. This means that the power required to keep constant the difference of temperature with respect to the reference cell decreases as the amount of injected air increases. The addition of a compound in the sample cell with higher heat capacity than that in the reference cell would result in a positive drift in the baseline. This was tested by experiments injecting water into cyclohexane (not shown). It is possible to take advantage of the baseline drift observed in our experiments to estimate the volume of air contained in the sample cell (see example in the Supplementary Material). This change in the baseline is not observed in the TA Instruments ITCs, most likely as the results of the different design of the sample cell, that being cylindrical will probably allow the release of air out of the measurement region during the titration experiment, at odds with what happens in the lollipop cells' shape in the MicroCal instrument.

To better understand the source of the different contributions to the power signal, we connected an analogic manometer to the injection system. This allowed us to observe on the flight the strong pressure changes due to the different stages in the bubble production: appearance at the tip of the capillary, growth, and releasing. This device does not form part of the standard design of the ITC instrument and the readings for the pressure change were not recorded but just used to identify the events that take place in the measurement cell at real time. The complementary information coming from ITC and pressure changes allowed us to identify three different regions in the raw power signal (Fig. 3). Region I was only detected at the beginning of the experiment. The corresponding power signal is weak, hardly distinguishable from the baseline, but it is present in all our experiments. During this stage, no bubble was formed and the manometer did not detect a significant pressure change, so it should correspond to a slow increase in pressure of the air contained in the syringe accompanied by a decrease in the level of liquid in the capillary and probably to some condensation at the small water/air interface of the meniscus. The initial height level of the solvent in the needle could be higher than that in the sample cell due to the capillary rise of the liquid. This explains why this contribution is detected only before the appearance of the first bubble. In contrast to region I, regions II and III were completely reproducible along the rest of the periodic profile. Our joint analysis of the pressure change and the calorimetric signal, complemented with the reproduction of the experiment outside of the ITC cell, in a transparent flask (Fig. 1) allowed us to identify the region II with the appearance and growth of the bubble at the tip of the capillary (see video in the Supplementary Material). Once the bubble appears, a quick expansion of the gas phase, accompanied by the increase of the liquid vapor interface area, takes place. Finally, Region III begins by the sharp peak associated with the delivery of the bubble, which is accompanied by the re-compression of the air (the pressure inside the syringe decreases when the bubble goes out) and the condensation of the vapor, as in region I. After this release, the cycle starts again but with a higher pressure than in the initial bubble, so the processes associated to region I are not appreciated for the rest of the bubbles. Additionally, there is a power contribution due to the bubble release strong perturbation. As stated above, the released bubble remains inside the sample cell displacing the corresponding volume of liquid, thus changing the total heat capacity of the sample cell. This provokes the baseline drift, as shown in the Supplementary Material.

6. Direct applications of the method

In the previous sections it has been shown that ITC instruments are able to detect a rich and highly reproducible power profile for the injection of air into water. In the present section we will show how it is possible to take advantage of this kind of experiments for different aims. The most obvious utility of the method is its use to extract thermodynamic, kinetic and mechanic information from the power profile. Next, we will show how that profile depends on the pure liquids located in the sample cell, how the period can be used to get accurate surface tension values for different liquids and samples, including biomacromolecules, and also how to use it in liquid-liquid interfaces.

6.1. Pure liquids and simple solutions

Water has an unusually high surface tension, so the volume of the bubbles formed in this liquid is abnormally high compared to that in other liquids with more ordinary surface tension values. In addition to water, the power profile for the continuous injection of air in ethanol, cyclohexane and EAN were registered (Fig. 4). As expected, the power profile is similar for all the compounds. The same contributions described above can be observed, although their magnitudes are different in each case. The correlation with the surface tension is clear not only in the period of the signal profile but also in the size (area or total heat) of some contributions, particularly in the negative peak associated to the release of the bubble from the capillary tip. Plainly, the periodic profile corresponding to each bubble contains a lot of useful information that deserves to be analyzed in detail. Although there are several phenomena involved in these experiments that lead to a significant heat exchange, they are not strongly coupled to each other and this facilitates the modeling of the signal. Ideally, we should be able to decouple the kinetic contribution of the molecular adsorption to the interface. From that contribution the surface tension could be directly obtained based on thermodynamic considerations, using a surface equation of state. The development of a model able to address this aim is currently in progress. Meanwhile, we focused on the period of the signal, that is expected to be clearly correlated to the bubble volume and therefore with the surface tension of the liquid in the sample cell. Beyond the pure liquid experiments, solutions with low concentration ethanol in water were also tested (Fig. 4). The addition of ethanol alters the bubble signal profile of water and the period decreases in a way that is proportional to the surface tension of the mixture, as expected.

6.2. Determination of surface tension

A number of different methods are commercially available to determine surface tension of liquids and liquid mixtures. Maximum drop volume tensiometers are based on a correlation between the maximum volume of a drop pending from a capillary and the surface tension, while maximum bubble pressure tensiometers use the maximum pressure of a bubble created in the bulk of a liquid phase for the same aim [25]. In our case, we get a periodic signal that can be exploited in a similar way. We propose to use the period as a direct observable to correlate with the surface tension of the studied liquid. The employed protocol has been described in detail in a recently registered patent [26]. This hypothesis was tested using different systems. First, we got the period for different pure liquids (see previous section) and then we got the period for a mixture of ethanol and $C_{10}G_2$ in water. High quality surface tension data obtained from a standard tensiometer are available in the literature, so the period as a function of the surface tension was plotted for all the studied concentrations at different injection rates. The behavior was completely linear, confirming our hypothesis (Fig. 5). Then we used just two pure compounds with extreme surface tension values (water for highest and ethanol or cyclohexane for lowest) as a reference and got the scaling factor to transform periods into surface tension values. The results are in excellent agreement with those obtained using standard surface tension instruments. The advantages of using ITC are clear: (*i*) isothermal calorimeters provide much more information than a standard tensiometer,; (*ii*) the required amount of sample is very low and it can be recovered at the end of the experiment since the injection of air do not contaminate it; (*iii*) the implementation of an additional injection system would allow changing the concentration of the sample cell with no need to open and clean it. This would also contribute to a considerable saving in time and sample. Additionally, ITC allows measuring properties for exactly the same solution both in the bulk and at the interface. Note that most experimental methods employed to characterize interfaces require specific setups and sample preparation, but it is not common to use exactly the same sample to perform measurements at both phases.

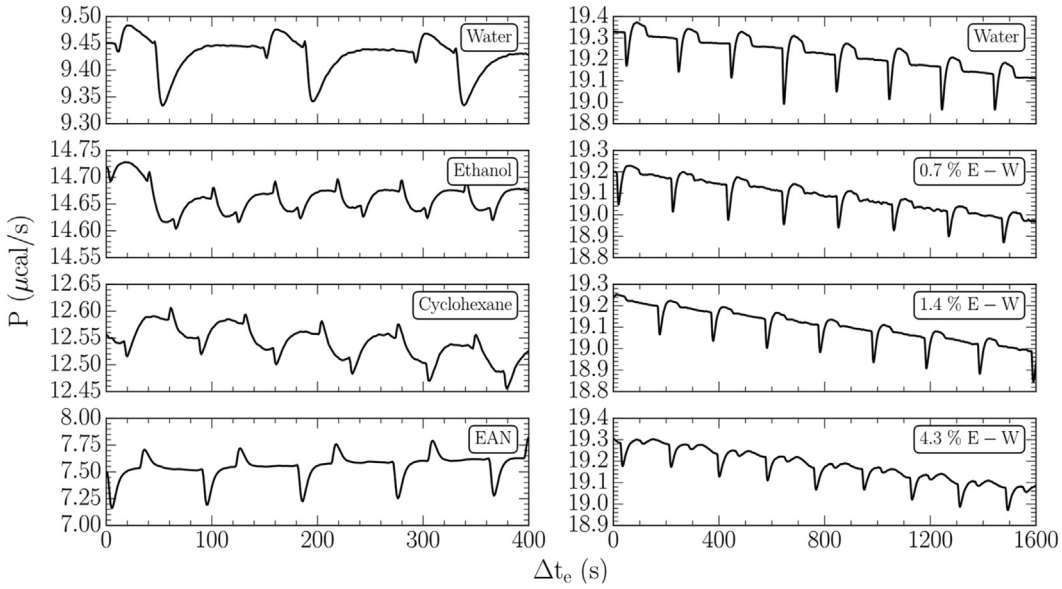

Fig. 4. Left: Experiments corresponding to the injection of air into water, ethanol, cyclohexane and ethylammonium nitrate using a reference power of 10, 20, 20 and 10 μcal/s, respectively, and an injection rate of 0.02 μL/s (100 μL injected in 4500 s). In all cases, a representative period of 400 s containing a minimum of 3 bubbles was selected. The power scale (ordinate axis) is the same for water, ethanol and cyclohexane (0.2 μcal/s), but not for EAN (1 μcal/s). Right: ITC experiments corresponding to the injection of air into different concentrations of ethanol in water using a reference power of 20 μcal/s and an injection rate of 0.02 μL/s (200 μL injected in 9000 s). Δt_e represents the elapsed time from the first point selected to plot along the titration experiments.

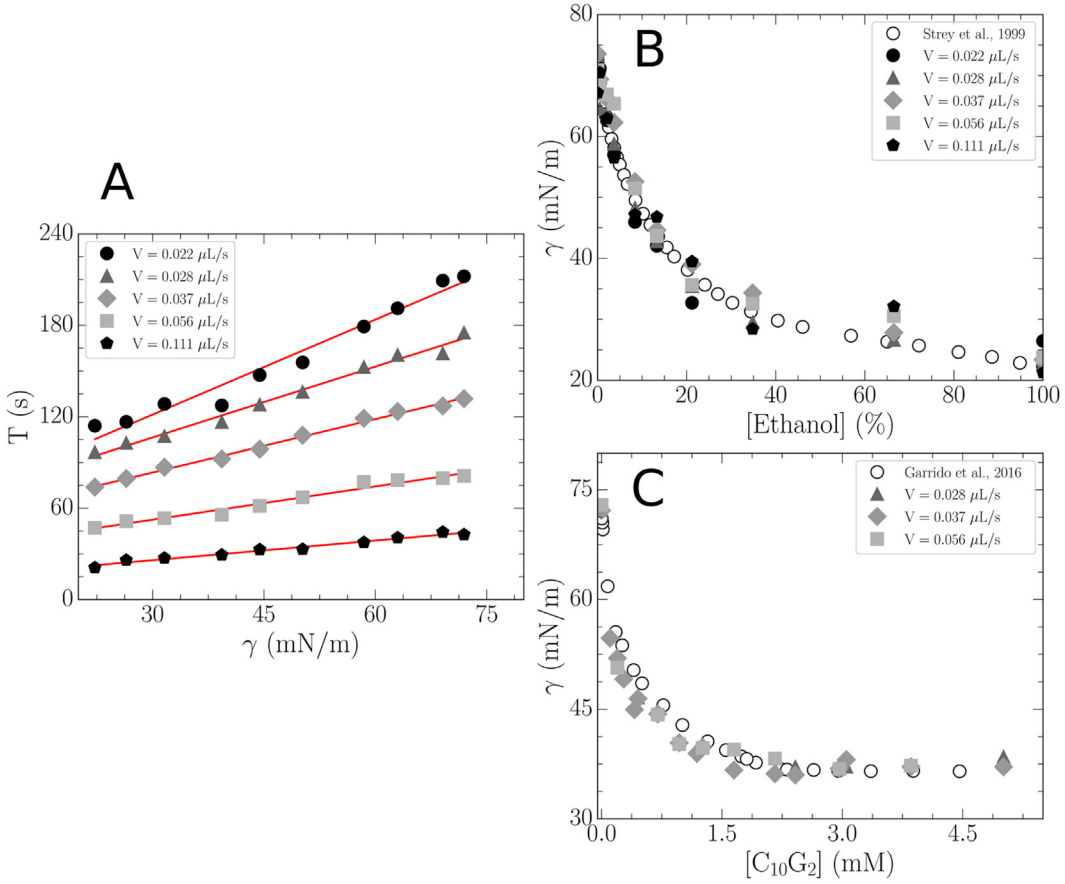

Fig. 5. Left: correlation between surface tension (γ) and period of bubble formation obtained for different concentrations of ethanol in water at different injection rates. Right: Surface tension values as a function of the concentration obtained for mixtures of ethanol and $C_{10}G_2$ in water, for different injection rates, compared with literature [27,28].

Similar experiments were performed using different concentrations of BSA in water. BSA is a globular protein with recognized surface activity [29]. It was observed that the period for bubble release clearly depends on the protein concentration (Fig. 6). However, since the adsorption of proteins is known to be relatively slow (in the time scale of tens of minutes or hours) due to its slow dif-

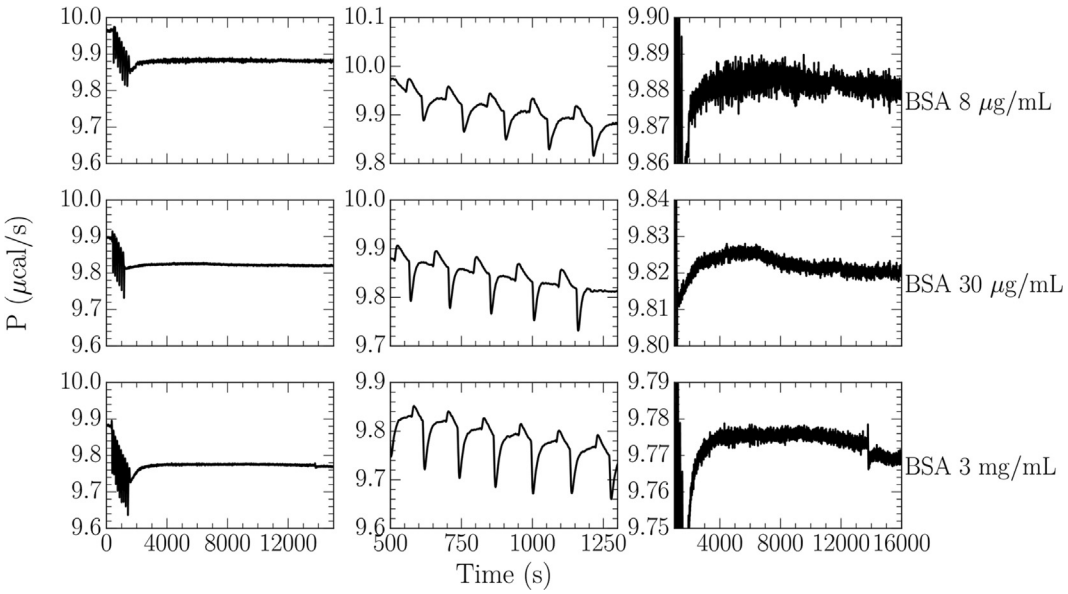

Fig. 6. Left: ITC experiments corresponding to the injection of 10 bubbles of air into different concentrations of BSA in water (see labels on the right of the plots), followed by 14,000 s of equilibration time to follow the signal corresponding to the potential adsorption of protein and to the recovering of the baseline. Middle and right: amplification on the titration and equilibration regions, respectively.

fusion, some additional experiments were performed by trying to stop the injection at a point where the bubble remains in the tip of the capillary. In this way, it should be possible to follow the kinetic signal of the protein adsorption process. These experiments present two main difficulties: (*i*) the injection should stop when the size of the bubble is significant in order to have enough surface area accessible for the adsorption of the protein to the liquid surface; (*ii*) the power exchanged is probably very low since we would measure the power associated to a slow process corresponding to the adsorption of large molecules to a relatively small area; and (*iii*) the dependence on the concentration should be carefully considered since the surface is expected to be quickly saturated at high concentrations of the macromolecule, so the kinetic signal should be negligible under those conditions, and (*iv*) the same point is expected to be slowly reached at too low concentrations due to the slow diffusion. The kinetic signal corresponding to these experiments at three different concentrations of BSA are shown in Fig. 6. Although the profile seems to depend on the protein concentration, the differences do not exhibit a clear trend. Altogether, our results for the experiments with proteins indicate that the method is definitely sensitive to the concentration, as revealed by the period (152 s for water or 149, 144 and 130 s for the 8 μg/mL, 30 μg/mL and 3 mg/mL BSA solutions, respectively), but some optimization in the instrument is still required to measure the adsorption kinetics.

6.3. Liquid-liquid interfaces

The previous method can be extrapolated to the characterization of liquid-liquid interfaces. Such interfaces only exist when using two immiscible liquids. The signal corresponding to the injection of water in cyclohexane was registered (Fig. S3). The liquid injected from the capillary forms a second phase which volume continuously grows in the sample cell. In this case no drops are formed and the water phase is always connected to the capillary. The signal raised linearly as a function of the amount of injected water. This behavior has been associated to the heat capacity change in the sample cell (see Supplementary Material). Additional experiments using different aqueous solutions of BSA instead of pure water completely saturated the signal, revealing that the instrument is really sensitive to the presence of protein. These experiments are promising, but they need to be optimized before producing useful information.

7. Conclusions and perspectives

In the present work it is conclusively shown that the heat corresponding to the formation of bubbles in a liquid solution can be detected by ITC and that the kinetic profile is perfectly reproducible between independent experiments and among different bubbles within the same experiment. The heat power signal showed to be extraordinarily rich in information, with contributions associated to different thermodynamic and dynamic processes, such as the creation of interfacial area, evaporation-condensation processes, pressure changes in the gas phases, heat exchange with the environment, bubble release and change in the heat capacity of the sample cell. It is also shown that the periodic heat power signal can be used as a new method to determine the surface tension of different liquids as well as for a given liquid as a function of the concentration of a solute. Moreover, the heat power associated to protein adsorption is registered for the first time, showing the versatility of our proposal. It is also shown that thermodynamics governs the signal, since the drop in the baseline upon air-injection was quantitatively connected to the change in heat capacity of the cell. This analysis was also useful to determine the amount of air contained in the cell at any point of the titration experiment. Overall, the new methodology presented in this work is based on the close connection between bulk solution and interfacial properties. Surface tension measurements have been used in the past to get the aggregation number of micelles in the bulk solution [6,27,30] and even association constants for the formation of supramolecular complexes [31]. No similar measurements are available for comparison since this is the first time that heat power corresponding to the formation of bubbles, and in general fluid-fluid interfacial experiments, are reported. However, the pressure profile of bubbles is well known and widely employed to measure surface tension of a variety of solutions [16]. Our results are in perfect agreement with typical maximum bubble pressure experi-

ments but it exhibits clear advantages and it has a lot of room for improvement. We are currently working on developing advanced kinetic and thermodynamic models to characterize these measurements. Although the experimental results shown in present work were obtained using unmodified instruments, we suggest that some modifications could greatly improve the quality and versatility of the measurements. For instance, by using the same model of calorimeter but different instruments, it is shown that small variations in the capillary shape and size have a large impact in the registered signal. Also, the introduction of complementary devices, such as pressure and optical sensors, would definitely help to understand the information provided by the heat power profile and so to design better experiments. There are also various possibilities for optimization in the injection system, not only in the geometry and size of the needle, but also in the introduction of an extra capillary to change the composition of the liquid in real time, or in the control of the injection rate with different patterns that could even depend on the real time pressure by a feedback system. The possibility to change the concentration of the liquid phase by using a second injection system would allow to efficiently measure the heat power associated to the surface adsorption of biomacromolecules as a function of their concentration, opening new possibilities in the characterization of protein conformational changes or protein association induced by interaction with interfaces, or even the spontaneous formation of biofilms. This is something of outstanding interest that has already been addressed by alternative computational and experimental methods [32–35].

Overall, in this work we present the first measurements of interfacial calorimetry. To our knowledge, the kinetic (power signal) and thermodynamic (heat associated to each contribution to the power profile) information provided by this method cannot be obtained by any other experimental technique. More practical applications are expected to arise from the proposed methodology.

CRediT authorship contribution statement

Pablo F. Garrido: Formal analysis, Investigation, Methodology, Validation, Writing. **Margarida Bastos:** Investigation, Methodology, Writing. **Adrián Velázquez-Campoy:** Investigation, Methodology, Writing. **Philippe Dumas:** Investigation, Methodology, Writing. **Ángel Piñeiro:** Conceptualization, Funding adquisition, Investigation, Methodology, Project administration, Writing.

Declaration of Competing Interest

The authors declare that they have no known competing financial interests or personal relationships that could have appeared to influence the work reported in this paper.

Acknowledgements

We would like to gratefully thank the help and support from Mike Brandts, from Malvern/Microcal, for the information provided on the basic properties of VP-ITC instruments, as well as from Malin Suurkuusk and Peter Vikegard, from Waters/TA Instruments, for allowing us to use the calorimeters available in their lab. The authors thank the financial support of the Spanish Ministry of Economy and Competitiveness (projects MAT2015-71826-P to Á. P. and BFU2016-78232-P to A.V.C.), the Agencia Estatal de Investigación (AEI) (project PID2019-111327GB-I00 to Á. P.) and Fundação para a Ciência e Tecnologia (FCT), Portugal, for CIQUP (project UIDB/00081/2020 to M.B.). P. F. G. thanks the Spanish Ministry of Economy and Competitiveness and the European Social Fund for his predoctoral research grant, reference BES-2016-076761. These research projects were partially supported by European ERDF Funds (MCIU/AEI/FEDER, EU). Facilities provided by the Galician Supercomputing Centre (CESGA) are also acknowledged.

Appendix A. Supplementary data

Supplementary data to this article can be found online at https://doi.org/10.1016/j.jcis.2021.03.098.

References

[1] J.E. Ladbury, M.L. Doyle, Biocalorimetry 2: Applications of Calorimetry in the Biological Sciences, John Wiley & Sons, Ltd, Chichester, UK, 2004. doi: 10.1002/0470011122.
[2] M. Textor, S. Keller, Calorimetric Quantification of Cyclodextrin-Mediated Detergent Extraction for Membrane-Protein Reconstitution, in: A.L. Feig (Ed.), Methods Enzymol., Elsevier, 2016, pp. 129–156. doi: 10.1016/bs.mie.2015.07.033.
[3] R.J. Falconer, Applications of isothermal titration calorimetry - the research and technical developments from, 2011 to 2015, J. Mol. Recognit. 29 (2016) 504–515, https://doi.org/10.1002/jmr.2550.
[4] T. Silva, B. Claro, B.F.B. Silva, N. Vale, P. Gomes, M.S. Gomes, S.S. Funari, J. Teixeira, D. Uhríková, M. Bastos, Unravelling a Mechanism of Action for a Cecropin A-Melittin Hybrid Antimicrobial Peptide: The Induced Formation of Multilamellar Lipid Stacks, Langmuir 34 (2018) 2158–2170, https://doi.org/10.1021/acs.langmuir.7b03639.
[5] A. Velazquez-Campoy, S.A. Leavitt, E. Freire, Characterization of Protein-Protein Interactions by Isothermal Titration Calorimetry, in: H. Fu (Ed.), Protein-Protein Interact. Methods Appl., Humana Press, Totowa, NJ, 2004, pp. 35–54. doi: 10.1385/1-59259-762-9:035.
[6] W. Loh, C. Brinatti, K.C. Tam, Use of isothermal titration calorimetry to study surfactant aggregation in colloidal systems, Biochim. Biophys. Acta - Gen. Subj. 2016 (1860) 999–1016, https://doi.org/10.1016/j.bbagen.2015.10.003.
[7] D. Burnouf, E. Ennifar, S. Guedich, B. Puffer, G. Hoffmann, G. Bec, F.F.F. Disdier, M. Baltzinger, P. Dumas, kinITC: A new method for obtaining joint thermodynamic and kinetic data by isothermal titration calorimetry, J. Am. Chem. Soc. 134 (2011) 559–565, https://doi.org/10.1021/ja209057d.
[8] P. Dumas, Joining thermodynamics and kinetics by kinITC, in: M. Bastos (Ed.), Biocalorimetry Found. Contemp. Approaches, CRC Press, 2016, pp. 281–300. doi: 10.1201/b20161.
[9] P. Dumas, E. Ennifar, C. Da Veiga, G. Bec, W. Palau, C. Di Primo, A. Piñeiro, J. Sabin, E. Muñoz, J. Rial, Extending ITC to Kinetics with kinITC, in: Methods Enzymol., Academic Press Inc., 2016, pp. 157–180. doi: 10.1016/bs.mie.2015.08.026.
[10] E. Muñoz, A. Piñeiro, AFFINImeter Software: from its Beginnings to Future Trends- A Literature review, J. Appl. Bioanal. 4 (2018) 124–139, https://doi.org/10.17145/jab.18.017.
[11] Á. Piñeiro, E. Muñoz, J. Sabín, M. Costas, M. Bastos, A. Velázquez-Campoy, P.F. Garrido, P. Dumas, E. Ennifar, L. García-Río, J. Rial, D. Pérez, P. Fraga, A. Rodríguez, C. Cotelo, AFFINImeter: A software to analyze molecular recognition processes from experimental data, Anal. Biochem. 577 (2019) 117–134, https://doi.org/10.1016/j.ab.2019.02.031.
[12] H. Zhao, G. Piszczek, P. Schuck, SEDPHAT - A platform for global ITC analysis and global multi-method analysis of molecular interactions, Methods 76 (2015) 137–148, https://doi.org/10.1016/j.ymeth.2014.11.012.
[13] S. Keller, C. Vargas, H. Zhao, G. Piszczek, C.A. Brautigam, P. Schuck, High-precision isothermal titration calorimetry with automated peak-shape analysis, Anal. Chem. 84 (2012) 5066–5073, https://doi.org/10.1021/ac3007522.
[14] S. Builes, S.I. Sandler, R. Xiong, Isosteric Heats of Gas and Liquid Adsorption, Langmuir 29 (2013) 10416–10422, https://doi.org/10.1021/la401035p.
[15] J. Juliš, Differential heats of adsorption, Chem. Pap. 29 (1975) 653–659.
[16] A. Javadi, N. Mucic, M. Karbaschi, J.Y. Won, M. Lotfi, A. Dan, V. Ulaganathan, G. Gochev, A.V. Makievski, V.I. Kovalchuk, N.M. Kovalchuk, J. Krägel, R. Miller, Characterization methods for liquid interfacial layers, Eur. Phys. J. Spec. Top. 222 (2013) 7–29, https://doi.org/10.1140/epjst/e2013-01822-3.
[17] S.S. Dukhin, G. Kretzschmar, R. Miller, Dynamics of adsorption at liquid interfaces: theory, experiment, application, Elsevier, Amsterdam, 1995.
[18] G. Bracco, B. Holst, Surface science techniques, Springer, Berlin, Heidelberg, 2013. doi: 10.1007/978-3-642-34243-1.
[19] J.M. Ruso, Á. Piñeiro (Eds.), Proteins in solution and at interfaces: methods and applications in biotechnology and materials science, John Wiley & Sons, Hoboken, New Jersey, 2013.
[20] M.K. Transtrum, L.D. Hansen, C. Quinn, Enzyme kinetics determined by single-injection isothermal titration calorimetry, Methods 76 (2015) 194–200, https://doi.org/10.1016/j.ymeth.2014.12.003.
[21] K.A. Vander Meulen, S.E. Butcher, Characterization of the kinetic and thermodynamic landscape of RNA folding using a novel application of isothermal titration calorimetry, Nucleic Acids Res. 40 (2012) 2140–2151, https://doi.org/10.1093/nar/gkr894.
[22] N.H. Yennawar, J.A. Fecko, S.A. Showalter, P.C. Bevilacqua, A High-Throughput Biological Calorimetry Core: Steps to Startup, Run, and Maintain a Multiuser Facility, in: Methods Enzymol., Academic Press Inc., 2016, pp. 435–460. doi: 10.1016/bs.mie.2015.07.024.

[23] C. Jesús, F. Socorro, M.R. De Rivera, New approach to Tian's equation applied to heat conduction and liquid injection calorimeters, J. Therm. Anal. Calorim. 110 (2012) 1523–1532, https://doi.org/10.1007/s10973-011-2117-1.
[24] K.J. Mysels, The maximum bubble pressure method of measuring surface tension, revisited, Colloids Surfaces 43 (1990) 241–262, https://doi.org/10.1016/0166-6622(90)80291-B.
[25] A.W. Adamson, A.P. Gast, Physical chemistry of surfaces, sixth ed., John Wiley & Sons, New York, 1997.
[26] P.F. Garrido, M. Bastos, Á. Piñeiro, Method for determining interfacial tension, WO2020043792A1, 2020. https://worldwide.espacenet.com/patent/search/family/067777338/publication/WO2020043792A1?q=pn%3DWO2020043792A1.
[27] P.F. Garrido, P. Brocos, A. Amigo, L. García-Río, J. Gracia-Fadrique, Á. Piñeiro, STAND: Surface Tension for Aggregation Number Determination, Langmuir 32 (2016) 3917–3925, https://doi.org/10.1021/acs.langmuir.6b00477.
[28] R. Strey, Y. Viisanen, M. Aratono, J.P. Kratohvil, Q. Yin, S.E. Friberg, On the Necessity of Using Activities in the Gibbs Equation, J. Phys. Chem. B. 103 (1999) 9112–9116, https://doi.org/10.1021/jp990306w.
[29] A. Berthold, H. Schubert, N. Brandes, L. Kroh, R. Miller, Behaviour of BSA and of BSA-derivatives at the air/water interface, Colloids Surfaces A Physicochem. Eng. Asp. 301 (2007) 16–22, https://doi.org/10.1016/j.colsurfa.2006.11.054.
[30] N.E. Olesen, R. Holm, P. Westh, Determination of the aggregation number for micelles by isothermal titration calorimetry, Thermochim. Acta 588 (2014) 28–37, https://doi.org/10.1016/j.tca.2014.04.028.
[31] Á. Piñeiro, X. Banquy, S. Pérez-Casas, E. Tovar, A. García, A. Villa, A. Amigo, A.E. Mark, M. Costas, S. Perez-Casas, E. Tovar, A. García, A. Villa, A. Amigo, A.E. Mark, M. Costas, On the characterization of host-guest complexes: Surface tension, calorimetry, and molecular dynamics, of cyclodextrins with a non-ionic surfactant, J. Phys. Chem. B 111 (2007) 4383–4392, https://doi.org/10.1021/jp0688815.
[32] C. Postel, O. Abillon, B. Desbat, Structure and denaturation of adsorbed lysozyme at the air-water interface, J. Colloid Interface Sci. 266 (2003) 74–81, https://doi.org/10.1016/S0021-9797(03)00571-X.
[33] M. Arooj, N.S. Gandhi, C.A. Kreck, D.W.M. Arrigan, R.L. Mancera, Adsorption and Unfolding of Lysozyme at a Polarized Aqueous-Organic Liquid Interface, J. Phys. Chem. B 120 (2016) 3100–3112, https://doi.org/10.1021/acs.jpcb.6b00536.
[34] Q. Kou, Z. Wu, N. Hu, Thermodynamic adsorption properties of bovine serum albumin and lysozyme on the bubble surface from the binary solution, Chem. Eng. Res. Des. 102 (2015) 26–33, https://doi.org/10.1016/j.cherd.2015.06.013.
[35] B.A. Noskov, A.A. Mikhailovskaya, S. Lin, G. Loglio, R. Miller, Bovine Serum Albumin Unfolding at the Air / Water Interface as Studied by Dilational Surface Rheology, Langmuir 26 (2010) 17225–17231, https://doi.org/10.1021/la103360h.